

# LANDAU FLUID MODEL OF MULTI-STREAM INSTABILITIES AND APPLICATION TO PLASMA CONTACTOR PLUMES

V. Lapuerta and E. Ahedo  
*E.T.S.I. Aeronáuticos, Univ. Politécnica, 28040 Madrid, Spain*

*Linear stability of the plasma structure in a contactor plume, which includes an intermediate DL, is here analyzed by formulating a macroscopic model that includes correctly the effects of Landau resonance. Different electrostatic instabilities can develop in the two different tree-species, quasineutral plasmas formed at both sides of DL. For large contactor potentials, it is found that the plume develops an electron-electron instability, whereas a radial ion-electron macroinstability of the Buneman type does not set up.*

## 1. INTRODUCTION

Plasma contactors, which attain a good electrical contact with a surrounding plasma by emitting an artificial plasma cloud, have been proposed as a suitable solution for space applications, like electrodynamic tethers and spacecraft charging control, where large electrical currents are required. This paper is focused in the study of the plasma plume outside an anodic (i. e. electron-collecting) contactor, that is an electron collector. For large plasma emissions this plume consists of two quasineutral regions separated by a space-charge double layer (DL) where most of the potential drop takes place, Fig. 1. The strong potential jump across the DL accelerates ambient electrons (species  $e$ ) to the high potential side (*core*), emitted ions ( $i$ ) to the low potential side (*presheath*), confines emitted electrons ( $c$ ) into the core and ambient ions ( $a$ ) into the presheath. Thus, two different three-species plasmas are formed at each side of DL: an electron-electron-ion (e-e-i) plasma at the core and an ion-ion-electron (i-i-e) plasma at the presheath.

Many experiments have detected plasma fluctuations of different frequencies at both sides of DLs [1]. The high-velocity beams created by the DL make current-driven instabilities as the most plausible cause of these fluctuations. Vannaroni *et al.* [1] discussed the presence of the ion-acoustic and bump-in-tail instabilities and concluded that the second one could explain the anomalous heating observed in their experiments. Other authors [2] have proposed the simultaneous development in the plasma plume of the Buneman and ion-acoustic instabilities. However, it is still an open question which particular type of instability set up, since those authors use classical results from two-species, homogeneous plasmas, whereas the plume around a plasma contactor, consists of two different three-species plasmas at both sides of the DL, with two populations drifting. Furthermore, the DL is a free-surface of discontinuity that introduces a strong spatial inhomogeneity and the plasmas at both sides of DL are inhomogeneous also. The two last issues make the problem very dif-

ficult to afford with a kinetic formulation. Indeed, a stationary solution is known only from a macroscopic model and a simplified geometry. On the other hand, the problem with a macroscopic model is how to include Landau resonance effects. This is important because several *microinstabilities* are due to Landau resonance (for instance, the ion-acoustic and bump-in-tail ones).

This paper summarizes our investigations on electrostatic instabilities in a plasma contactor plume. The paper is divided in three parts:

(i) The formulation of a macroscopic model of linear, electrostatic perturbations in an homogeneous plasma, which includes correctly the effects of Landau resonance [Section 2].

(ii) The analysis of electrostatic instabilities in three-species plasmas of the types formed at both DL sides [Section 3].

(iii) The stability analysis of a whole stationary solution with an intermediate DL [Section 4].

## 2. LANDAU FLUID MODEL IN A PLANAR GEOMETRY

The dynamics of each plasma species is modeled by the following macroscopic equations:

$$\frac{\partial n_\alpha}{\partial t} + \nabla \cdot (n_\alpha \vec{V}_\alpha) = 0, \quad (1)$$

$$m_\alpha \left( \frac{\partial \vec{V}_\alpha}{\partial t} + (\vec{V}_\alpha \cdot \nabla) \vec{V}_\alpha \right) + q_\alpha \nabla \phi + \frac{\nabla p_\alpha}{n_\alpha} = 0, \quad (2)$$

$$p_\alpha \equiv n_\alpha T_\alpha = p_\alpha(n_\alpha) \quad (3)$$

where:  $\alpha = i, e, a, c$  is representing each species;  $\phi$  is the electric potential and  $\vec{V}_\alpha$ ,  $n_\alpha$ ,  $p_\alpha$ ,  $m_\alpha$  and  $q_\alpha = \pm e$  mean macroscopic velocity, density, pressure, particle mass and electric charge; and  $p_\alpha(n_\alpha)$  is the thermodynamic law required to close the fluid model.

An exact closure law, with Landau resonance included, is known only for the most basic case of linear perturbations on a planar, homogeneous plasma. The steady solution consists of  $\phi_0$ ,  $\vec{V}_{\alpha 0}$  and  $n_{\alpha 0}$  constant and the perturbation solution is a linear combination of modes proportional to  $\exp(ikx - i\omega t)$ , with

$\vec{k} = k\vec{1}_x$ . Refs. [3] and [4] show that the linear perturbation problem admits the following formulation:

$$(\omega - kV_{\alpha 0})n_{\alpha 1} = n_{\alpha 0}kV_{\alpha 1}, \quad (4)$$

$$(\omega - kV_{\alpha 0})m_{\alpha}n_{\alpha 0}V_{\alpha 1} = k(q_{\alpha}n_{\alpha 0}\phi_1 + p_{\alpha 1}), \quad (5)$$

$$p_{\alpha 1} = \gamma(z_{\alpha})T_{\alpha 0}n_{\alpha 1}. \quad (6)$$

with  $kV_{\alpha 0,1} \equiv \vec{V}_{\alpha 0,1} \cdot \vec{k}$ ,

$$z_{\alpha} = \frac{\omega - kV_{\alpha 0}}{kc_{\alpha 0}},$$

$c_{\alpha 0} = \sqrt{T_{\alpha 0}/m_{\alpha}}$  is the thermal speed and

$$\gamma(z) = z^2 + \frac{1}{R(z)}, \quad (7)$$

where  $R(z)$  is the density response function, which, for  $z$  real, is convenient to express as  $R(z) = R_1(z) + iR_2(z)$ , with [5]

$$R_1(z) = 1 - z \exp(-z^2/2) \int_0^z \exp(y^2/2) dy, \quad (8)$$

$$R_2(z) = \sqrt{\pi/2} z \exp(-z^2/2). \quad (9)$$

Notice that, for  $z$  real,  $R_2$  is just the Landau resonance effect. Using these expressions, the pressure coefficient  $\gamma$  is decomposed in real and imaginary components

$$\gamma_1(z) = z^2 + \frac{R_1(z)}{|R(z)|^2}, \quad \gamma_2(z) = \frac{R_2(z)}{|R(z)|^2}. \quad (10)$$

Figure 2 depicts them as functions of  $z$ . Eq. (10) shows that  $\gamma_2$  is due uniquely to Landau resonance and, that, the two limits,  $z \rightarrow 0$  and  $z \rightarrow \infty$  correspond to the isothermal ( $\gamma = 1$ ) and adiabatic ( $\gamma = 3$ ) response, respectively.

From Eq. (4) and (6) we rewrite the closure law as:

$$p_{\alpha 1} = \gamma_1(z_{\alpha})n_{\alpha 1}T_{\alpha 0} - i\gamma_2'(z_{\alpha})m_{\alpha}n_{\alpha 0}c_{\alpha 0}V_{\alpha 1},$$

with  $\gamma_2' = \gamma_2/z_{\alpha}$ . This law separates the non-dissipative and dissipative components of the total pressure. The dissipative part is proportional to  $R_2$ , which indicates the existence of an anomalous resistivity associated to Landau resonance.

### 3. INSTABILITY MODES IN MULTI-STREAM PLASMAS

The macroscopic model, Eqs.(4)-(6), together with Poisson equation for the electrostatic perturbation potential

$$\epsilon_0 k^2 \phi_1 = \sum_{\alpha} q_{\alpha} n_{\alpha 1}, \quad (11)$$

form a closed equation system. For a given plasma, eigenmodes are the solution  $\omega(k)$  from the linear dispersion relation:

$$D(k, \omega) \equiv 1 + \sum_{\alpha} \frac{\omega_{p\alpha}^2}{k^2 c_{\alpha 0}^2 \gamma_{\alpha} - (\omega - kV_{\alpha 0})^2} = 0, \quad (12)$$

with  $\gamma_{\alpha} \equiv \gamma(z_{\alpha})$ ,  $\lambda_{D\alpha}^2 = \epsilon_0 T_{\alpha 0} / q_{\alpha}^2 n_{\alpha 0}$ , and  $\omega_{p\alpha} = c_{\alpha 0} / \lambda_{D\alpha}$ .

For the linear-stability analysis we follow the temporal theory and look for solutions  $\omega = \omega(k)$  of the dispersion relation for  $k$  real (and positive) and  $\omega = \omega_{re} + i\omega_{im}$  complex; unstable modes in Eq. (12) correspond to  $\omega_{im} > 0$ . For each stationary solution, the characteristics of the most unstable mode will be represented by an asterisk:  $\omega_{im}^*$ ,  $z_{\alpha}^*$ , etcetera.

#### 3.1. Instabilities in an e-e-i plasma

We consider the e-e-i plasma of the core, which consists of a quiescent electron population(*c*), an electron beam(*e*) of velocity  $\vec{V}_{e0}$ , and an ion beam(*i*) of velocity  $\vec{V}_{i0}$ . Plasma quasineutrality implies  $n_{i0} = n_{e0} + n_{c0}$ . The solutions of the dispersion relation (12) depend mainly on three dimensionless parameters:  $n_{e0}/n_{c0}$ ,  $V_{e0}/c_{e0}$ ,  $T_{e0}/T_{c0}$ ; two other parameters,  $V_{i0}/V_{e0}$  and  $T_{i0}/T_{c0}$  are assumed small.

In the long-wavelength limit,  $k\lambda_{D\alpha} \rightarrow 0$ , modes develop in three different frequency ranges [4]: i) one pair of Langmuir modes at  $\omega \sim \omega_p = \sqrt{\omega_{pe}^2 + \omega_{pc}^2}$ , ii) one pair of e-e (acoustic) modes at  $\omega \sim kV_{e0}$ , and iii) one pair of i-e (acoustic) modes at  $\omega \sim kV_{e0}\sqrt{m_e/m_i}$ . Instabilities come from the i-e and e-e modes. Figure 3 shows the maximum growth rate of the i-e and e-e instabilities in terms of  $V_{e0}/c_{e0}$  and  $n_{c0}/n_{e0}$ . There are, in general, one i-e and one e-e unstable modes, with one of them clearly dominant except in the transition domain. To understand these results, let us discuss first some properties of the i-e and e-e unstable modes.

For i-e modes, dropping inertia effects for electrons, Eq. (12) yields,

$$\left(\frac{\omega}{k} - V_{i0}\right)^2 = \frac{c_{s0}^2}{k^2 \lambda_{De}^2 + S - iR_2(V_{e0}/c_{e0})}, \quad (13)$$

with

$$S \equiv R_1(V_{e0}/c_{e0}) + \Lambda^{-1}, \quad \Lambda = \frac{\lambda_{Dc}^2}{\lambda_{De}^2} \equiv \frac{n_{e0}T_{c0}}{n_{c0}T_{e0}},$$

and  $c_{s0} = c_{e0}\sqrt{m_e/m_i}$ . Eq. (13) shows that the character of the i-e instability depends mainly on the sign of  $S$ : If  $S > 0$ , the only instability source is the term with  $R_2$ , so the instability is *resistive*, caused by Landau resonance. If  $S < 0$  and  $|R_2/S| \ll 1$ , the instability is *reactive* (i.e. hydrodynamic) with

negligible Landau effect. The instability is of mixed type for  $S < 0$  and  $|R_2/S| \geq O(1)$ .

For  $\Lambda \rightarrow \infty$ , Eq.(13) is valid for  $V_{e0}/c_{e0} \leq O(1)$ . For  $V_{e0}/c_{e0} > 3.4$ , small non-steady effects on electrons must be retained and, for  $V_{e0}/c_{e0} \gg 1$ , the i-e instability becomes the Buneman instability with:

$$\frac{\omega_{im}^*}{\omega_{pe}} \simeq \frac{3^{1/2}}{2^{4/3}} \left( \frac{m_e}{m_i} \right)^{1/3}. \quad (14)$$

For e-e modes, ions remain quasi-rigid. The e-e instability is classified into the *strong-beam* instability for  $n_{e0}/n_{c0} = O(1)$ , and the *weak-beam* instability for  $n_{e0}/n_{c0} \ll 1$  (or  $n_{e0}/n_{c0} \gg 1$ , due to symmetry). Depending on the drift velocity, and for  $T_{e0}/T_{c0} = O(1)$ , the weak-beam case is subclassified into the *bump-in-tail* instability, for  $c_{e0} \ll V_{e0} \ll c_{e0}(n_{c0}/n_{e0})^{1/3}$ , with

$$\frac{\omega_{im}^*}{\omega_{pe}} \simeq \frac{V_{e0}^2}{2c_{e0}^2} \left[ \frac{n_{e0}}{n_{c0}} R_2(1) - \frac{T_{e0}}{T_{c0}} R_2 \left( \frac{V_{e0}}{c_{e0}} \right) \right], \quad (15)$$

and the *cold weak-beam* instability, for  $c_{e0}(n_{c0}/n_{e0})^{1/3} \ll V_{e0}$ , with [6, 7]

$$\frac{\omega_{im}^*}{\omega_{pe}} \simeq \frac{3^{1/2}}{2^{4/3}} \left( \frac{n_{e0}}{n_{c0}} \right)^{1/3}. \quad (16)$$

The weak-beam instability is reactive in the cold-plasma limit (as the Buneman instability) and it is Landau-resistive in the bump-in-tail limit.

From the above expressions, the dominant instability mode depends on  $n_{e0}/n_{c0}$ :

– Case 1:  $0 < n_{e0}/n_{c0} \ll m_i/m_e$ , Fig. 3(a). The e-e instability is clearly dominant within, practically, its whole domain of existence. Below that domain, the plasma presents a resistive i-e instability with a maximum of  $\omega_{im}^*$  for an intermediate value of  $V_{e0}/c_{e0}$ . The i-e instability decays sharply when it interacts with the e-e instability and there is no trace of the reactive, Buneman instability for  $V_{e0}/c_{e0} \gg 1$ .

– Case 2:  $m_i/m_e \ll n_{e0}/n_{c0}$ , Figure 3(b). The e-e instability is very weak and the i-e instability is dominant for any  $V_{e0}/c_{e0}$ . The transition region between cases 1 and 2 is obtained from Eqs. (14) and (16).

Figure 4 summarizes the parametric regions of dominance for each type of instability. In regions I-III different forms of the e-e instability dominate, while in regions IV-VI different forms of the i-e instability are dominant. Notice that, in an e-e-i plasma a reactive i-e instability exists in a very limited region with  $n_{e0}/n_{c0} \gg 1$ , while the typical case in plasma contactor double-layers is just the opposite one:  $n_{e0}/n_{c0} \ll 1$ . When  $T_{e0}/T_{c0}$  decreases, the region of i-e resistive instability increases. For  $T_{i0}/T_{c0} = O(1)$ , the domain of existence of the i-e instability is restricted to  $V_{e0}/c_{e0} \geq 1$ .

### 3.2. Instability modes in an i-i-e plasma

We consider now the i-i-e plasma of the presheath, which consists of a quiescent ion population (*a*), an electron beam (*e*) of velocity  $\bar{V}_{e0} > 0$ , and an ion beam (*i*) of velocity  $\bar{V}_{i0} < 0$  (ion and electron beams are counterstreaming); plasma quasineutrality implies  $n_{e0} = n_{i0} + n_{a0}$ . The solutions of (12) depend mainly on three parameters:  $n_{i0}/n_{e0}$ ,  $V_{e0}/c_{e0}$ ,  $V_{i0}/c_{i0}$ ; two other parameters,  $T_{a0}/T_{e0}$  and  $T_{i0}/T_{e0}$ , are assumed small.

For large wavelength limit,  $k\lambda_{D\alpha} \rightarrow 0$ , there develop: one pair of Langmuir modes, mounted on the *e*-beam at  $\omega \sim \omega_{pe}$ ; and, depending on the drift velocities [4, 8]:

a) For  $V_{e0}/c_{e0} \ll V_{i0}/c_{s0}$ , two pairs of i-e acoustic modes at  $\omega \sim kV_{i0}$  and  $\omega \sim kV_{e0}(m_e/m_i)^{1/2}(n_{a0}/n_{e0})^{1/2}$ . Here, the *e*-beam interacts separately with the two ion populations, and produces two independent pairs of i-e modes.

b) For  $V_{e0}/c_{e0} \gg V_{i0}/c_{s0}$ , there are one pair of i-e acoustic modes at  $\omega \sim kV_{e0}\sqrt{m_e/m_i}$  and one pair of i-i acoustic modes at  $\omega \sim kV_{i0}$ . In the i-e pair, the high-velocity *e*-beam sees the two ion populations as a single one, and the interaction yields the classical i-e modes of a two-species plasma. The i-i pair corresponds to the residual interaction between the two ion populations at a lower frequency. These i-i modes present similarities with the e-e modes.

Instabilities come from both i-e and i-i modes. Figure 5 shows the maximum growth rate of the two unstable modes in terms of  $V_{e0}/c_{e0} > 0$  with  $V_{i0}/c_{s0} < 0$  [counterstreaming beams]. Notice that:

(i) There are two unstable modes in the whole velocity range.

(ii) For  $V_{e0}/c_{e0} \ll V_{i0}/c_{s0}$ , the two lines correspond to two i-e unstable modes, as predicted.

(iii) For  $V_{i0}/c_{s0} \ll V_{e0}/c_{e0}$ , the i-e instability dominates over the i-i instability (curve 2). The ratio  $n_{i0}/n_{a0}$  affects the i-i instability only, and  $\omega_{im}^*$  is maximum for  $n_{i0}/n_{a0} = 1$ .

### 4. STABILITY ANALYSIS OF THE CONTACTOR PLUME

Finally, we analyze the stability of the whole stationary plasma structure around an anodic contactor. A macroscopic, dynamic version of the stationary spherical model of Ahedo *et al* [9] is used. The contactor is a sphere of radius  $R$ , biased to a high potential  $\phi_R$ , which emits an artificial plasma into a quiescent, unmagnetized plasma (subscript  $\infty$ ); let  $I_i$  be the emitted ion current. The ratio  $\lambda_{D\infty}/R$ , is considered small enough to follow a two-scale analysis, where the plasma is assumed quasineutral everywhere except in the DL, which is treated as a free discontinuity in the quasineutral scale (related

to  $R$ ). Plasma dynamics are represented by Eqs. (1)-(3). Poisson equation simplifies to the quasineutral condition  $\sum q_\alpha n_\alpha = 0$ , in core and presheath, and yields jump and transition conditions at the DL. These include a generalized Langmuir condition for the plasma currents and the Bohm condition.

The stationary model determines the electron current collected,  $I_{e0}$ , the DL position  $r_{D0}$ , the potential jump across the DL,  $\Delta\phi_{0D}$ , and the plasma profiles in terms of  $\phi_{0R}$ ,  $I_{i0}$ , and the rest of plasma parameters.

The spherical version of the planar perturbation model, Eqs. (4)-(6), is

$$i\omega n_{\alpha 1} - \frac{1}{r^2} \frac{\partial}{\partial r} (r^2 n_{\alpha 1} V_{\alpha 0} + r^2 n_{\alpha 0} V_{\alpha 1}) = 0, \quad (17)$$

$$i\omega m_\alpha V_{\alpha 1} - \frac{\partial}{\partial r} (m_\alpha V_{\alpha 0} V_{\alpha 1} + q_\alpha U_1) = \frac{1}{n_{\alpha 0}} \frac{\partial p_{\alpha 1}}{\partial r}, \quad (18)$$

$$p_{\alpha 1} = \hat{\gamma}_\alpha T_{\alpha 0} n_{\alpha 1}, \quad (19)$$

where  $\hat{\gamma}_\alpha(V_{e0}/c_{e0}, \dots)$  in Eq. (19) must be a function independent of  $\omega/k$ . The most plausible choice is to take  $\hat{\gamma}_\alpha$  equal to  $\gamma(z_\alpha^*)$  of the instability mode under consideration.

There are, at least, two distinguished ranges for the frequencies of the perturbation modes: (i) *ion frequencies*,  $\omega \sim R^{-1} \sqrt{T_\infty/m_i}$ , when the electron response is quasisteady, and plasma dynamics are based in i-e and i-i modes; and (ii) *electron frequencies*,  $\omega \sim R^{-1} \sqrt{T_\infty/m_e}$ , when ions stay rigid in their stationary response, and plasma dynamics are dominated by e-e modes.

For ion frequencies, assuming  $T_{i0} = 0$  and  $T_{a0} \sim T_{e0}$ , we take [4]:

$$\hat{\gamma}_i \simeq 3, \quad \hat{\gamma}_a \simeq \gamma(V_{e0}/c_{e0}), \quad \hat{\gamma}_c \simeq 1, \quad \hat{\gamma}_e \simeq \gamma(-V_{e0}/c_{e0}). \quad (20)$$

For electron frequencies, assuming  $n_{e0} \ll n_{c0}$  (weak-beam limit), ion equations are not needed and we propose to use [4]:

$$\hat{\gamma}_c \simeq \gamma(V_{e0}/c_{c0}), \quad \hat{\gamma}_e \simeq \gamma(-V_{e0}/c_{c0}). \quad (21)$$

Equations (17)-(19) together with quasineutrality condition form a system of ordinary differential equations for each  $\omega$ . As boundary conditions for this system we have: i) the solution is bounded in all the space; ii) the jump and transition conditions at the DL; iii) perturbations are zero at  $r = \infty$ ; and iv) perturbations on conditions at the contactor exhaust are specified:  $I_{i1R}$ ,  $V_{c1R}$ ,  $\dots$ . The displacement of the DL,  $r_{D1}$  is part of the solution.

The perturbation equations are integrated from  $r = \infty$  to  $r = R$ , solving separately the presheath and the core. The general solution of Eqs. (17)-(19) is a combination of fundamental modes and, imposing to them the set of conditions at both boundaries,

we obtain an algebraic relation:  $AX = B$ , where  $A$  depends on the steady solution,  $X$  are the unknown parameters of the fundamental perturbation modes and  $B$  depends on the boundary conditions parameters. For  $B \neq 0$  we obtain regular dynamic responses. Self-excited modes for  $B = 0$  exist if and only if

$$\det A \equiv D\left(\omega; \frac{r_{D0}}{R}, \frac{\phi_{0R}}{T_\infty}, \dots\right) = 0, \quad (22)$$

for any  $\omega$  value. Therefore  $D = 0$  is the dispersion relation of the problem, which depends on  $\omega$  and the parameters of the steady solution.

Perturbations at the contactor surface are transmitted along the core by acoustic modes. When these modes reach the DL, they perturb its pressure balance and this produces a perturbation of the flow of incoming electrons. Furthermore, the DL is displaced itself and its displacement induces the motion of the ambient ions, which results in acoustic outward modes in the presheath. Therefore, the dynamic response of the core/DL/presheath structure is the combination of electron-electron, ion-electron and ion-ion modes, with different characteristics in core and presheath.

For a high contactor potential [ $e\phi_{0R}/T_\infty \gg 1$ ] we have  $V_{e0}/c_{e0} \gg 1$ , and we can take  $\hat{\gamma}_\alpha$  constant and real. For this case, the analysis for homogeneous plasmas in Section 3 suggests that the strongest instability is the e-e weak-beam instability. This is confirmed by the stability analysis of the contactor plume structure that has shown the presence of a reactive electron-electron macroinstability. Figure 6 shows the spatial-temporal response of the electric potential,  $\phi(r, t) = \phi_0(r) + \phi_1(r, t)$ , for an unstable mode. At the core the plasma response is a combination of two stationary modes and two e-e acoustic modes, mounted on the  $e$  beam for  $n_{e0}/n_{c0} \ll 1$ . For a purely oscillatory perturbation ( $\omega_{im} = 0$ ) only the acoustic mode propagating inwards (from the e-beam) is amplified. The ion rigidity in this frequency range produces a barrier effect that freezes the DL displacement. At the presheath there is a negligible i-e mode and a quasisteady one.

There are different branches of e-e unstable modes which correspond to different harmonics. The maximum growth rate, bounded by space charge effects, is

$$\frac{\omega_{im}^*}{\omega_{pe}} \sim \left(\frac{n_{e0}}{n_{c0}}\right)^{1/3},$$

which is of the order of the maximum value given by Eq. (16). The instability decreases when  $R/r_{D0}$ ,  $T_{c0}/T_\infty$  or  $e\phi_{0R}/T_\infty$  decrease; it disappears for  $e\phi_{0R}/T_\infty = O(1)$ .

For ion frequencies, Ref. [10] showed the non-existence of any radial, ion-electron macroinstability

of the global plasma structure, including the no generation of the Buneman instability, as the analysis in Sec. 3.1 predicted already.

Figure 7 shows the regular spatial-temporal response of the electric potential for a purely oscillatory perturbation on the emitted current  $I_{iR}$ . Now, the plasma response at the core is a combination of two traveller i-e acoustic modes with opposite velocities with respect to the ion beam frame, and one quasisteady e-e mode. At the presheat there is an ion acoustic and an electron standing mode.

Here, only the reactive instabilities have been study since we have used  $\hat{\gamma}_\alpha$  real for all the species. To study the resistive instabilities we should use  $\hat{\gamma}_\alpha$  from Eqs.(20)-(21). At core and presheath, only the ion-acoustic (micro)instability is likely, since unstable modes have been detected by the local dispersion relation for the parametric range of these regions.

## 5. CONCLUSIONS

This work has presented, first, a macroscopic model of linear, electrostatic perturbations which includes correctly the effects of Landau resonance. This model has then been applied to investigate the instability modes of the e-e-i and i-i-e plasmas. For an e-e-i plasma it is found that the i-e instability growth rate decays sharply when it starts to coexist with the e-e instability, which is dominant within, practically, its whole domain of existence. The reactive i-e instability is dominant in a very limited region with  $n_{e0}/n_{c0} \gg 1$ . For an i-i-e plasma there develop either two i-e instability modes or one i-e and one i-i instability mode, depending on the drift velocities.

Finally, the stability analysis of a whole stationary structure of a plasma plume around an anodic plasma contactor, with an intermediate DL has been presented. The main conclusions of the stability analysis are (i) the existence of an e-e cold weak-beam instability; (ii) the non-existence of any radial, ion-electron macroinstability of the global plasma structure, including the no generation of the Buneman instability. This conclusion refutes the analyses

of Refs. [2], which assert the generation, in the core, of the Buneman (macro)instability, together with an ion-acoustic (micro)instability. Indeed, the presence at the core of one pair of i-e modes and one pair of e-e modes made unlikely the simultaneous presence of two i-e unstable modes.

## References

- [1] J.D. Williams and P. J. Wilbur. *J. Spacecraft*, 27:634–641, 1990; G. Vannaroni, M. Dobrowolny, E. Melchioni, F. de Venuto, and R. Giovi. *J. Appl. Phys.*, 71:4709–4717, 1992.
- [2] D.E. Hastings and N.A. Gatsonis. *Acta Astronautica*, 17:827–836, 1988; A. Gioulekas and D.E. Hastings. *J. Propulsion and Power*, 6:559–566, 1990.
- [3] P. Stubbe and I. Sukhorukov, *Physics of Plasmas* **6**, 2976 (1999).
- [4] E. Ahedo and V. Lapuerta. *submitted to Phys. Plasmas*.
- [5] S. Ichimaru. *Statistical Plasma Physics*. Addison-Wesley Publishing Company, Redwood City, 1992.
- [6] A. Krall and A. Trivelpiece. *Principles of Plasma Physics*. San Francisco Press, San Francisco, 1986.
- [7] D. B. Melrose. *Instabilities in Space and Laboratory Plasmas*. Cambridge University Press, Cambridge, 1986.
- [8] V. Lapuerta. *Phd Tesis: Non uniformities and linear stability of spheric contactors in unmagnetized plasmas*. E.T.S.I.Aeronáuticos, 1998.
- [9] E. Ahedo, J.R. Sanmartín, and M. Martínez-Sánchez. *Phys. Fluids B*, 4:3847–3855, 1992.
- [10] V. Lapuerta and E. Ahedo. *Physics of Plasmas*, 7:2693–, 2000.

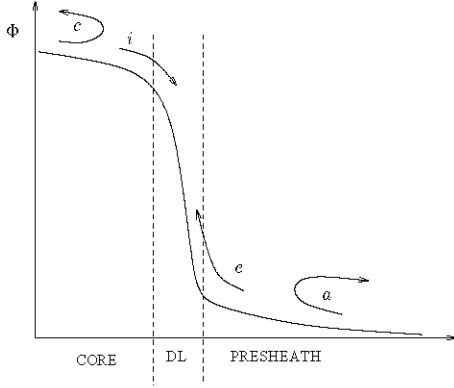


**Figure 1.-** Sketch of axial profile of the electrostatic potential in a plasma structure with intermediate DL.

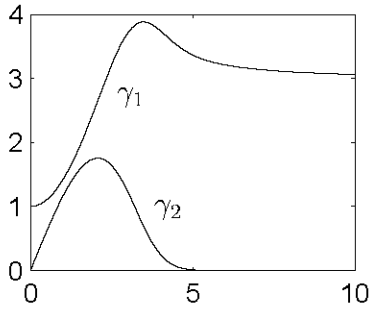


**Figure 2.-** Transport coefficients  $\gamma_1(z)$  and  $\gamma_2(z)$  for  $z$  real.

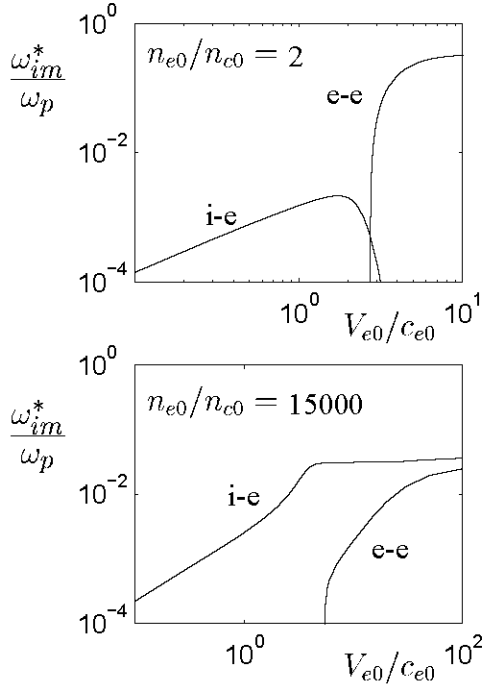


**Figure 3.-** Evolution of  $\omega_{im}^*$  with  $V_{e0}/c_{e0}$ . Other parameters:  $T_{e0} = T_{c0}$ ,  $m_e/m_i = 10^{-4}$ .

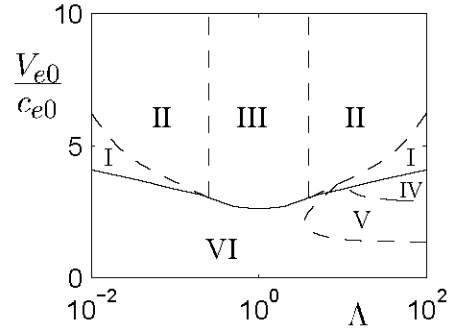


**Figure 4.-** Parametric regions of the different stability types in an e-e-i plasma: (I) Bump-in-tail, (II) e-e cold weak-beam, (III) e-e strong-beam, (IV) i-e reactive, (V) i-e mixed, (VI) i-e resistive.

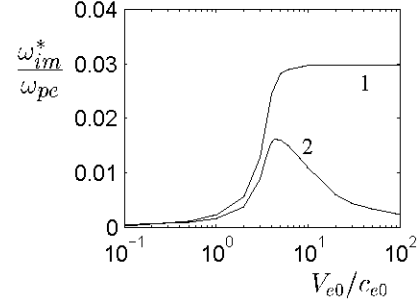


**Figure 5.-** Evolution of  $\omega_{im}^*$  with  $V_{e0}/c_{e0}$  for  $n_{i0}/n_{e0} = 0.2$  and  $V_{i0}/c_{s0} = -30$ ;  $m_e/m_i = 10^{-4}$ .

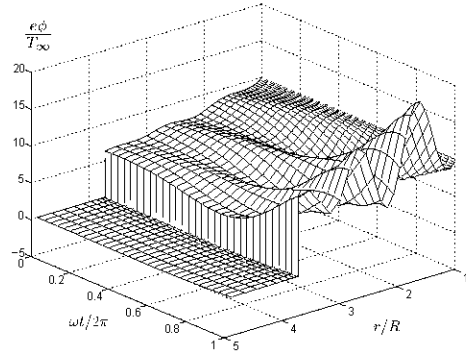


**Figure 6.-** Spatial-temporal response of electric potential for an e-e unstable mode [8].

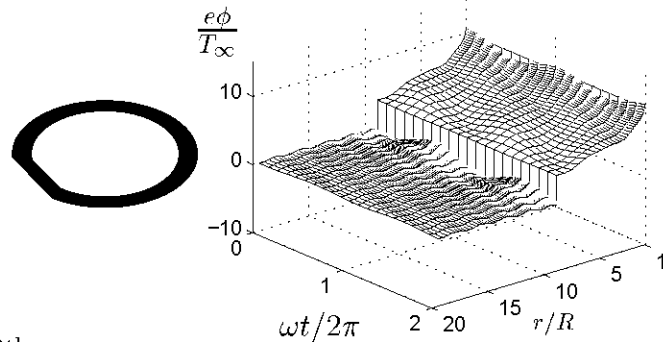


**Figure 7.-** Spatial-temporal response of electric potential for an oscillatory perturbation  $I_{i1R}$  [10].